LETTER

TM Scattering from a Dielectric-Loaded Semi-Circular Trough in a Conducting Plane

Tah J. PARK†, Hyo J. EOM†, Wolfgang-M. BOERNER††
and* Yoshio YAMAGUCHI†††, *Members

SUMMARY The behavior of TM-wave scattering from a dielectric-loaded semicircular trough in a conducting half-space is investigated. The dielectric loading is made of a circular cylinder which lies in a semi-circular trough in the perfectly conducting plane. The formulation is numerically evaluated to investigate the scattered field pattern for various dielectric loading conditions. It is found that the scattering patterns exhibit the resonant behavior due to both of the concave surface contour and the dielectric loading.

key words: *rough surface scattering*

1. Introduction

In the study of random rough surface scattering, a great deal of theoretical investigation have been done to better understand the scattering process from rough surface boundaries. The rough surface boundaries may be classified into two different types, namely the concave and the convex. The rough surface which contain the convex (protrusions) above the mean surface may be dealt with effectively with the image theory[(1),(2)], but this is not the case for the concave surface (depressed below the mean surface). For instance, in order to deal with scattering from a cavity-backed gap, pit, or crack in the perfectly conducting plane, a low frequency approximation or an integral equation formulation[(3)-(5)] have been used. In this paper we study how incident wave interacts with the depressed concave surface of *a semi-cirular trough with a dielectric loading*. Electromagnetic scattering behavior from a dielectric-loaded semi-circular trough was first investigated in Ref. (6) with the technique of approximated series expansions. Unlike approximated approach which is valid for only low frequency ranges, we solve the boundary value problem of TM-wave scattering from such a concave surface, using the tangential E and H field continuity conditions. A similar mathematical approach was used in Ref. (7) to study the scattering behavior of a dielectric-absent semicircular channel in the perfectly conducting plane. In the next section, the theoretical formulations are presented and numerical computations are performed to show the angular scattering behavior.

Manuscript received April 11, 1991.
Manuscript revised July 18, 1991.

† The authors are with the Department of Electrical Engineering Korea Advanced Institute of Science and Technology 400, Kusung-dong, Yusung-gu, Taejon, Korea.
†† The author is with the Department of Electrical Engineering and Computer Science, University of Illinois at Chicago, Chicago, IL 60680, USA.
††† The author is with the Faculty of Engineering, Niigata University, Niigata-shi, 950-21 Japan.

2. Scattered Field Representation

Throughout the paper, $e^{j\omega t}$ time harmonic factor is suppressed. Assume that a TM^y plane wave is incident upon a dielectric-loaded trough in a perfectly-conducting half-space. The dielectric of a circular shape with radius a and wave number k_1 is loaded in a trough as shown in Fig. 1. When the incident wave impinges on the trough in the half-space, a surface scattering process takes place, resulting in scattered, specularly reflected, and transmitted field as follows:

In region II$(\rho > a, 0 < \phi < \pi)$, the total field may be decomposed into three parts, the incident, the reflected, and the scattered fields, $E_y^i(\rho, \phi)$, $E_y^r(\rho, \phi)$, and $E_y^s(\rho, \phi)$, respectively:

$$E_y^i(\rho, \phi) = \exp[jk\rho[\cos(\phi - \phi_0)]]$$

$$= \sum_{m=0}^{\infty} \varepsilon_m (j)^m J_m(k\rho) \cos m(\phi - \phi_0)$$

where

$$\varepsilon_m = 1 \quad m = 0$$

$$\varepsilon_m = 2 \quad m = 1, 2, 3, \cdots$$

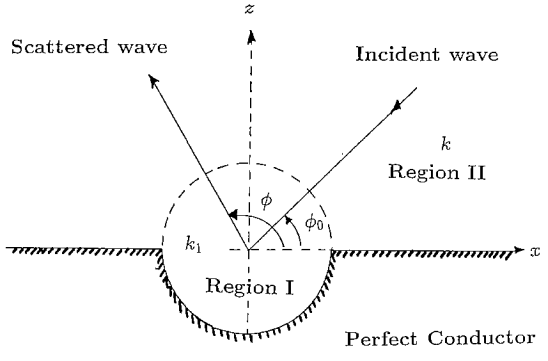

Fig. 1 Geometry of surface scattering problem.

J_m: Bessel function of mth order

k: wave number in region (II)

$$E_y^r(\rho, \phi) = -\exp[jk\rho\cos(\phi+\phi_0)]$$

$$= -\sum_{m=0}^{\infty} \varepsilon_m (j)^m J_m(k\rho)\cos m(\phi+\phi_0)$$

$$E_y^s(\rho, \phi) = \sum_{m=0}^{\infty} A_m \sin m\phi H_m^{(2)}(k\rho)$$

where $H_m^{(2)}$ is the Hankel function of the mth order and the second kind.

In region (I), $(\rho < a, 0 < \phi < 2\pi)$, the transmitted field may be represented as

$$E_y^t(\rho, \phi) = \sum_{m=0}^{\infty} (B_m \cos m\phi + C_m \sin m\phi) J_m(k_1\rho)$$

In the above equations, A_m, B_m, C_m are unknown Fourier coefficients yet to be determined with the boundary conditions.

First, the tangential E-field ontinuity at $\rho = a$, and $0 < \phi < \pi$, requires that

$$E_y^i(a, \phi) + E_y^r(a, \phi) + E_y^s(a, \phi) = E_y^t(a, \phi)$$

which may be rewritten as

$$\sum_{m=0}^{\infty} 2\varepsilon_m (j)^m J_m(ka)\sin m\phi_0 \sin m\phi$$

$$= \sum_{m=0}^{\infty} [B_m J_m(k_1 a)\cos m\phi + [C_m J_m(k_1 a) - A_m H_m^{(2)}(ka)]\sin m\phi]$$

Multiplying the above equation by $\sin n\phi$ and integrating the both sides with respect to ϕ from 0 to π, we obtain for $n \geqq 1$

$$\pi\varepsilon_n (j)^n J_n(ka)\sin n\phi_0$$

$$= \sum_{\substack{m=0 \\ n+m=\text{odd}}}^{\infty} B_m J_m(k_1 a)\frac{2n}{(n^2-m^2)} + [C_n J_n(k_1 a) - A_n H_n^{(2)}(ka)]\pi/2 \qquad (1)$$

where $\sum_{n+m=\text{odd}}$ represents a summation over m which satisfies $n+m=\text{odd}$.

In a similar fashion, the enforcement of the tangential H-field continuity at $\rho = a$ and $0 < \phi < \pi$, yields the following simultaneous equation for A_n, B_n, C_n, for $n \geqq 1$.

$$\pi\varepsilon_n (j)^n k J_n'(ka)\sin n\phi_0$$

$$= \sum_{\substack{m=0 \\ n+m=\text{odd}}}^{\infty} B_m k_1 J_m'(k_1 a)\frac{2n}{(n^2-m^2)} + [C_n k_1 J_n'(k_1 a) - A_n k H_n^{(2)\prime}(ka)]\pi/2 \qquad (2)$$

where J_n' and $H_n^{(2)\prime}$ denote the differentiation of the respective Bessel functions with respect to the argument.

Now, we need to enforce the boundary condition of the tangential E-field continuity at $\rho = a$ and $\pi < \phi < 2\pi$.

$$\sum_{m=0}^{\infty} (B_m \cos m\phi + C_m \sin m\phi) J_m(k_1 a) = 0$$

Multiplying the above equation by $\cos n\phi$ and integrating the both sides with respect to ϕ from π to 2π, we have

$$B_n \frac{\pi}{2} J_n(k_1 a) + \sum_{\substack{m=0 \\ n+m=\text{odd}}}^{\infty} \frac{2m}{(n^2-m^2)} C_m J_m(k_1 a) = 0, \quad n \geqq 1 \qquad (3)$$

$$B_0 \pi J_0(k_1 a) + \sum_{m=1}^{\infty} C_m J_m(k_1 a)[(-1)^m - 1]/m = 0, \quad n = 0 \qquad (4)$$

Rewriting the simultaneous equations for A_n, B_n, C_n (Eqs. (1) through (4)) in a matrix form,

$$\begin{bmatrix} a_{11} & a_{12} & a_{13} \\ a_{21} & a_{22} & a_{23} \\ 0 & a_{32} & a_{33} \end{bmatrix} \begin{bmatrix} A \\ B \\ C \end{bmatrix} = \begin{bmatrix} b_1 \\ b_2 \\ 0 \end{bmatrix}$$

The explicit expressions for the matrices are given:

$$a_{11} = -0.5\pi H_n^{(2)}(ka)$$

$$a_{12} = \frac{2n}{(n^2-m^2)} J_m(k_1 a)|_{n+m=\text{odd}}$$

$$a_{13} = 0.5\pi J_n(k_1 a)$$

$$a_{21} = -0.5\pi k H_n^{(2)\prime}(ka)$$

$$a_{22} = \frac{2n}{(n^2-m^2)} k_1 J_m'(k_1 a)|_{n+m=\text{odd}}$$

$$a_{23} = 0.5\pi k_1 J_n'(k_1 a)$$

$$a_{32} = 0.5\pi J_n(k_1 a), \quad n \geqq 1$$

$$a_{32} = \pi J_0(k_1 a), \quad n = 0$$

$$a_{33} = \frac{2m}{(n^2-m^2)} J_m(k_1 a)|_{n+m=\text{odd}}, \quad n \geqq 1$$

$$a_{33} = J_m(k_1 a)[(-1)^m - 1]/m, \quad n = 0$$

$$b_1 = \pi\varepsilon_n (j)^n J_n(ka)\sin(n\phi_0)$$

$$b_2 = \pi\varepsilon_n (j)^n k J_n'(ka)\sin(n\phi_0)$$

Note that a_{11}, a_{13}, a_{21}, a_{23} are $(n \times n)$ diagonal matrices, and a_{22}, a_{12} are $(n \times (1+n))$ full matrices, and a_{32} is an $((n+1) \times (n+1))$ diagonal matrix, and a_{33} is an $((n+1) \times n)$ full matrix, and A, C, b_1, b_2 are $(1 \times n)$ column matrices, and B is $(1 \times (n+1))$ column matrix, respectively.

It is possible to solve the above equation for A, B, C numerically for an arbitrary size of the trough; however, for a small-sized trough, an approximated closed form solution for the scattered field expression is also possible. For small ka $(ka \ll 1)$ case, it is

expedient to expand the Hankel and Bessel functions in terms of power series of ka and retain the first leading terms such as:

$$J_0(ka)\approx 1,\ J_1(ka)\approx ka/2,\ H_1^{(2)}(ka)\approx 2j/(\pi ka)$$

Substituting the above approximations in the matrix equation, and rearranging the equation, we come up with the low-frequency approximated equations for A_1, B_0, C_1, where the rest of A_n, B_n, C_n turn out to be zero, and

$$A_1=(ka)^2\sin\phi_0\frac{4}{(\pi+4/\pi)}\approx(ka)^2\sin\phi_0$$

$$C_1=\pi jk\sin\phi_0/[k_1(\pi/2+2/\pi)]$$

$$B_0=C_1k_1a/\pi$$

These results reveal that, for a very small irregularity above the plane, scattered field has a Rayleigh scattering pattern which is known as$\sim(ka)^2\sin\phi$.

In the next section, we examine the far zone scattered field behavior for different trough sizes, and frequency.

3. Scattered Field Computation

With the formulation developed in the previous section, it is possible to evaluate the scattered field from a dielectric-loaded trough on the perfectly conducting plane. In the numerical computation, the number of the Fourier series components must be kept finite but sufficiently large enough to achieve the series convergence and numerical accuracy. In order to see the rate of the series convergence, 15 Fourier components A_m are shown in Table 1 for $ka=5$ and 10 where $\phi_0=90°$ and $k=k_1$. Note that even components of A_m, i.e., $A_0=A_2=A_4\cdots=0$. The series convergence is, in fact, determined by the size of ka, meaning that the larger ka is, the more terms are needed in Fourier series expansion for better accuracy. Table 1 indicates that 15-term Fourier series expansion is adequate enough to achieve an accuracy to better than 1 percent in the far-zone scattered field computation. It is also very interesting to see how fast the Fourier series converge in the transmitted field computation which requires B_m and C_m. Figure 2 depicts the behavior of $|B_mJ_m(k_1\rho)|$ versus $k_1\rho$ when $ka=5$, $\phi_0=90°$, and $k=k_1$. It is seen that as m increases, $|B_mJ_m(k_1\rho)|$ becomes smaller. Note that odd components of B_m, i.e., $B_1=B_3=B_5\cdots=0$. Higher-order terms ($m=12, 14, \cdots$) are not shown since they are negligible in magnitude.

Figure 3 shows the behavior of the normalized scattered field magnitude $|P_e|$ versus ka for three different scattering angles, $\phi=90°$, 60°, 30° at normal incidence ($\phi_0=90°$) with $k_1=k$. The normalized scattered field magnitude $|P_e|$ means the far-zone scattered field amplitude which may be defined as $|P_e|=\sqrt{\pi k\rho/2}\,|E_y^s(\rho,\phi)|$. We first compare our result of backscattering (solid line, $\phi=90°$) with the low-

Table 1 Comparison of A_m for $ka=5$ and $ka=10$.

	A_m	
m	$ka=5$	$ka=10$
1	0.6819 - j 3.9209	-0.7124 - j 0.0805
3	1.5004 - j 4.3706	0.8422 + j 0.0562
5	0.5354 - j 1.3207	-0.1975 - j 4.3154
7	0.0816 - j 0.1840	-0.3144 - j 4.8011
9	0.0070 - j 0.0419	-0.0404 - j 2.2144
11	(0.3889 - j 0.7885) × 10^{-3}	0.0203 - j 0.5863
13	(0.0152 - j 0.0296) × 10^{-3}	0.0087 - j 0.1025
15	(0.0004 - j 0.0008) × 10^{-3}	0.0017 - j 0.0128

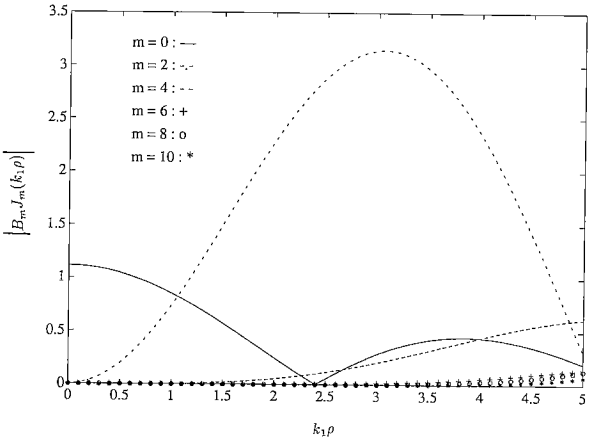

Fig. 2 Behavior of $|B_mJ_m(k_1\rho)|$ vs. $k_1\rho$.

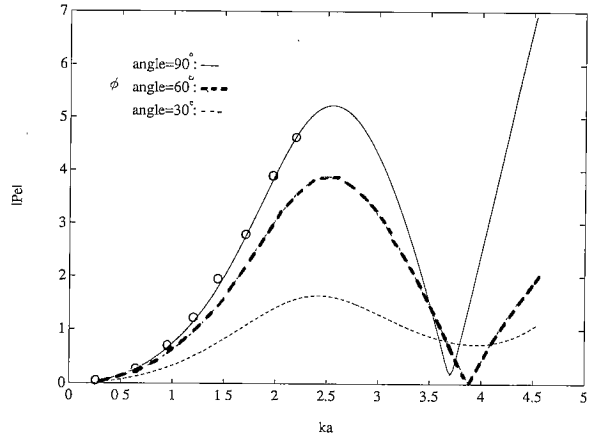

Fig. 3 Scattered field magnitude vs. ka for a vacant trough.

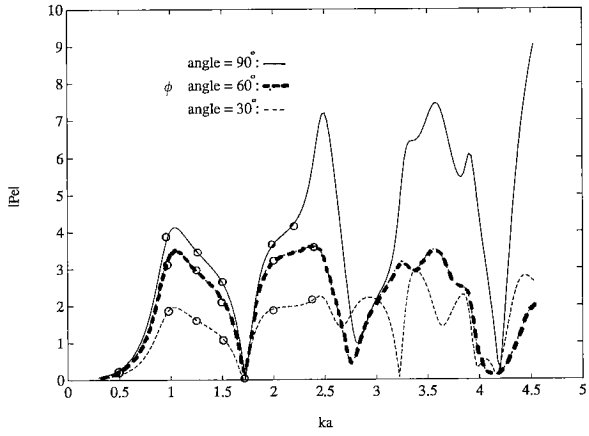

Fig. 4 Scattered field magnitude vs. ka for a dielectric-filled trough.

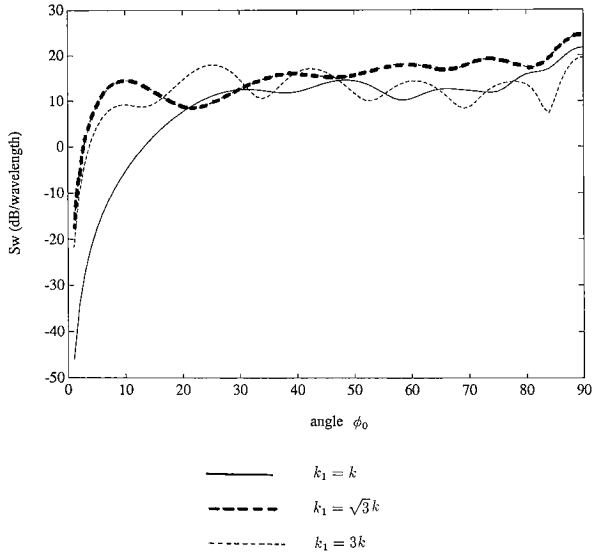

Fig. 5 Backscattering width vs. incident angles for three dielectric loadings.

frequency approximated one (○ ○ ○) which is available from[6]. Two results agree well for $ka<2.4$ which is the range of validity of the low-frequency solution in Ref. (6). A strong resonance behavior is shown to exist for all scattering angles. The resonance in scattering may be attributed to the multiple scattering process which undergoes inside the trough of the concave surface. Figure 4 shows the behavior of $|P_e|$ versus ka for three different scattering angles, $\phi=90°$, 60°, 30° at normal incidence ($\phi_0=90°$) when $k_1=\sqrt{3}k$. The agreement with the low-frequncy solution[6] (shown by symbols, '○ ○ ○ ') is shown to be excellent for $ka<$ 2.4. In view of Figs. 3 and 4, it is seen that a presence of the dielectric loading tends to decrease a period of the resonance versus ka. Figure 5 shows the back-

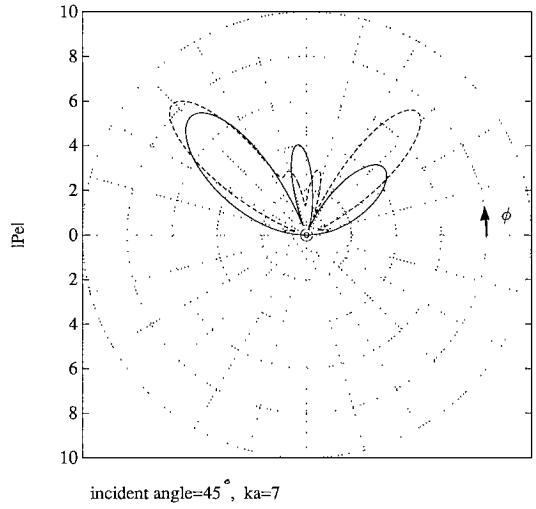

Fig. 6 Scattered field magnitude vs. ϕ for vacant (solid curve) and dielectric-fiilled (dotted curve) troughs.

scattering width versus the incident angles ϕ_0 for three different dielectric loading conditions, $k_1=k$, $k_1=\sqrt{3}k$, $k_1=3k$ and $ka=4\pi$. The backscattering width is defined as

$$S_w=\lim_{\rho\to\infty} 2\pi\rho|E_y^s(\rho, \phi_0)/E_y^i(\rho, \phi_0)|^2$$

The scattering pattern for $k_1=k$ case agrees exactly with the computed results in Ref. (8). It is clearly seen that the presence of the dielectric loading in the trough enhances the resonant scattering pattern. Note that a similar conclusion was drawn in Ref. (6). In Fig. 6, $|P_e|$ is plotted versus the scattering angle ϕ when $\phi_0=45°$, $ka=7$. The solid and dotted curves depict cases corresponding to $k_1=k$ and $k_1=15/7k$, respectively. It is seen that the main and side lobes exist in the forward and backward directions respectively.

4. Conclusions

The mathematical formulation for TM-scattering from a dielectric-filled circular trough is presented and numerical computations for scattered fields are shown. The numerical results agree well with the low-frequency solution[6] when $ka<2.4$. The resonant scattering pattern is shown to exist due to scattering from the concave surface contour and dielectric loading both. The formulation is simple to use so that it may not only help us understand the scattering behavior from a semi-circular trough, but also provide a means to crosscheck with other arbitrarily-shaped cavity scattering results.

Acknowledgment

The authors wish to thank Mr. M. K. Hinders and Dr. A. D. Yaghjian for kindly providing us their work

(Ref. (8)) for the purpose of crosschecking.

References

(1) Wirgin A. : "Resonance scattering from an arbitrarily shaped protuberance on a ground plane" Optica Acta, **22**, 1, pp. 47-58 (1975).

(2) Gray E. P., Hart R. W. and Farrel R. A. : "An application of variational principle for scattering by random rough surface", Radio Science, **23**, pp. 333-348 (1978).

(3) Senior T. B. A. and Volakis J. L. : "Scattering by gaps and cracks", IEEE Trans. Ant. and Propagat., **AP-37**, 6, pp. 744-750 (June 1989).

(4) Senior T. B. A., Sarabandi K. and Natzke J. R. : "Scattering by a narrow gap", IEEE Trans. Ant. & Propagat., **AP -38**, 7, pp. 1102-1110 (July 1990).

(5) Jin J.-M. and Volakis J. L. : "TM scattering by an inhomogeneously filled aperture in a thick conducting plane", IEE Proc., **137**, Pt.H, 3, pp. 153-159 (June 1990).

(6) Sachdeva B. K. and Hurd R. A. : "Scattering by a dielectric loaded trough in a conducting plane", J. Appl. Phys., **48**, 4, pp. 1473-1476 (April 1977).

(7) Hinders M. K. : "Scattering of a plane electromagnetic wave from a semicircular crack in a perfectly conducting ground plane", RADC Tech. Rept. TR-89-12, RADC, Griffiss AFB, NY 13441, USA (April 1982).

(8) Hinders M. K. and Yaghjian A. D. : "Dual series solution to scattering from a semicircular channel in a ground plane", IEEE Microwave and Guided Wave Letters, **1**, 9, pp.239-242 (Sept. 1991).